

# Copper-catalyzed cyclopropanation reaction of but-2-ene

Beatriz Angulo<sup>1</sup> · Clara I. Herrerías<sup>1</sup> · Zoel Hormigón<sup>1</sup> · José Antonio Mayoral<sup>1</sup> · Luis Salvatella<sup>1</sup>

✉ Luis Salvatella  
[lsalvate@unizar.es](mailto:lsalvate@unizar.es)

<sup>1</sup> Instituto de Síntesis Química y Catálisis Homogénea (ISQCH), CSIC–Universidad de Zaragoza, Pedro Cerbuna 12, E-50009 Zaragoza, Spain

## Abstract

The mechanism of the copper(I)-catalyzed cyclopropanation reaction for methyl diazoacetate with both (*Z*)- and (*E*)-but-2-ene stereoisomers has been studied using the 6-311++G(d,p) basis set by means of M06-2X and O3LYP functionals. According to both methods, the rate-limiting step is the formation of a copper-carbene intermediate, formed by association between methyl diazoacetate and bis(acetonitrile)-copper(I) ion with the concomitant extrusion of dinitrogen. *cis/trans* Diastereoselectivity for the cyclopropanation reaction of a 1,2-disubstituted alkene ((*Z*)-but-2-ene) has been theoretically studied for the first time through the proper location of transition states on the potential-energy surface with the O3LYP method, since no transition structures could be found with the M06-2X functional due to the extreme flatness of the potential-energy surface. The calculated stereoselectivities involving two acetonitrile ligands or one dichloromethane molecule show qualitative agreement with experimental data. This study allows attributing the origin of the selectivity to steric interactions between the ligands of the catalyst system and the olefin substituents. The comparison between the corresponding activation barriers for the direct insertion step shows a higher reactivity for the *Z* stereoisomer of but-2-ene, consistently with the larger reactant destabilization through steric interactions.

**Keywords:** Reaction mechanisms, Cyclopropanation, Copper, Catalysis, Stereoselective synthesis

## Electronic Supplementary Material

The online version of this article contains supplementary material (experimental details, energies and Cartesian coordinates of all structures), which is available to authorized users.

## Acknowledgements

Allocation of computer time is thanked to the Instituto de Síntesis Química y Catálisis Homogénea (ISQCH) and the Instituto de Biocomputación y Física de Sistemas Complejos (BIFI) (Consejo Superior de Investigaciones Científicas (CSIC)–Universidad de Zaragoza). Financial support from Ministerio de Economía y Competitividad (MINECO) (Project CTQ2014-52367-R), Gobierno de Aragón, European Regional Development Fund (Consolidated Group E11), and European Social Fund is gratefully acknowledged.

## 1 Introduction

Cyclopropane derivatives constitute an important family of chemical compounds with interesting properties from both biological and synthetic viewpoints [1,2]. Thus, research has focused in the development of efficient highly diastereo- and enantioselective methods for the synthesis of cyclopropanes [3–5]. Among them, a common and versatile procedure is the metal-catalyzed decomposition of diazo compounds in the presence of olefins, for which various efficient catalysts have been developed [6].

Copper-based catalysts are particularly attractive due to their high efficiency in asymmetric cyclopropanation reactions [7] and their relatively low cost in comparison with other metal catalysts. In order to gain better understanding of the stereoselectivity governing factors, and thereby upgrade the ability to design more efficient catalytic systems, the mechanism of the copper-catalyzed cyclopropanation reaction of olefins with diazo compounds has been experimentally [6] and theoretically [8] studied in recent years, and the pathway for the global catalytic cycle is now well established. Thus, it is agreed that the active catalyst is a Cu(I) species, irrespective of the oxidation state of the copper complex used as the precatalyst, since Cu(II) complexes are reduced to Cu(I) derivatives by diazo compounds under the reaction conditions [9].

Furthermore, it is accepted that the rate-limiting step of the copper-catalyzed cyclopropanation reaction is the formation of a copper-carbene intermediate, formed by association of the diazo compound and the catalyst with the concomitant dinitrogen extrusion [9–11]. Since carbene insertion occurs after this step, the stereochemical product distribution is governed by the cyclopropane ring formation step, which proceeds via direct carbene insertion, according to several theoretical studies conducted to rationalize the stereochemical outcome of the copper-catalyzed cyclopropanation reaction [8].

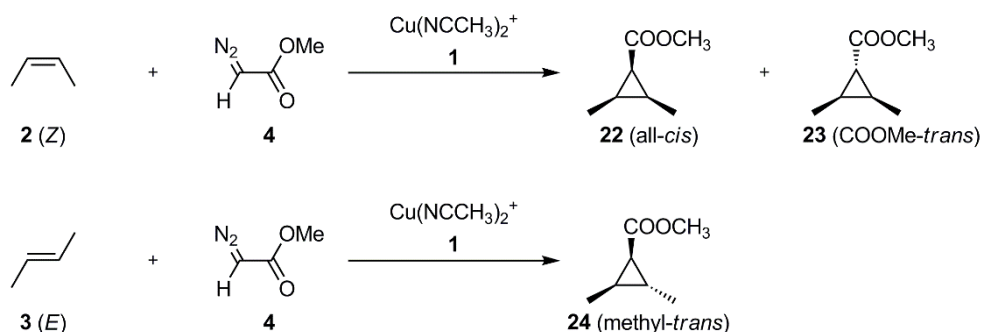
Most of previous theoretical studies on cyclopropanation reactions catalyzed by copper(I) complexes were conducted using ethylene [11–14] or propene [11] as simple olefin models. Instead, no transition states (TS) have been located on the potential energy surface (PES) of typical theoretical methods for the reaction involving styrene (a common reactant in experimental studies) or related species, presumably due to its high reactivity [14–16]. As a matter of fact, the PES for the cyclopropanation reactions of cationic ligand-Cu-carbene complexes is indeed very flat, as reported by Norrby and coworkers [17] and thoroughly confirmed by our group [18], which makes the detection of activation barriers of the cyclopropanation reaction, except for computational methods derived from Handy's OPTX exchange functional [19,20], only possible on the (estimated) Gibbs free-energy surface (GFES), which is extremely difficult to calculate for complex systems.

Our research group is currently interested on the chemical valorization of fatty acid derivatives [21,22]. In particular, our aim is to study the cyclopropanation reaction of oleic acid derivatives with diazoacetic esters in order to obtain branched fatty acid derivatives with useful properties (lower viscosity, larger biodegradation resistance, use as cross-linkers). For the sake of a rational design of such a process, we present here the first theoretical study on the *cis/trans* diastereoselectivity of the Cu(I)-catalyzed cyclopropanation reaction for 1,2-disubstituted alkenes [14,16]. In this work, a detailed mechanistic study of the copper-catalyzed cyclopropanation reaction of methyl diazoacetate with both *E* and *Z* isomers of but-

2-ene, by means of Density Functional Theory (DFT) calculations, is presented. The bis(acetonitrile)-copper(I) cation was regarded as a reactive and realistic catalyst model, consistently with the stabilization of such a complex in low permittivity solvents [23]. Nevertheless, a dichloromethane-coordinated copper(I) cation was also considered for stereoselectivity calculations. In this study, the nature of reaction intermediates and transition states, and *cis/trans* selectivity will be discussed for the first time for (*Z*)-but-2-ene by quantum mechanical methods.

## 2 Methods

A comprehensive mechanistic study of the copper-catalyzed cyclopropanation reaction was carried out by means of a model including a number of simple reactants: bis(acetonitrile)-copper(I) cation (denoted as **1**) as the catalyst, but-2-ene (**2** for *Z* stereoisomer, **3** for *E* isomer) as the olefin, and methyl diazoacetate (**4**) as the diazo compound (Scheme 1). A copper-carbene complex is involved in the catalytic cycle as a key reaction intermediate. The subsequent ring formation (through a concerted mechanism named as direct carbene insertion) is assumed, since no TS could be found for an alternative path involving a metallacyclobutane intermediate [11]. *cis/trans* Selectivity has been discussed by comparison of the relative energies of the transition structures for (*Z*)-but-2-ene. All possible conformations were taken into account for every structure, though the discussion of the results is centered on the most stable form in each case.



**Scheme 1** Cu-Catalyzed Cyclopropanation Reactions

Calculations were carried out by using the Gaussian package (versions A.02 [24] and D.01 [25]). Full optimizations for all structures were carried out by means of the hybrid *meta*-generalized M06-2X [26] (as well as the M06-2X/D3 method for two structures) and hybrid generalized gradient O3LYP [19] functionals by using the default integration grid. The 6-311++G(d,p) basis set was used for all atoms since excellent results have been obtained for the computed properties of some copper derivatives by using that basis set [27,28]. The wavefunction stability for each calculated TS was ensured by means of the keyword STABLE. No Basis Set Superposition Error corrections were considered throughout this work.


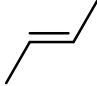
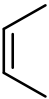
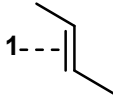
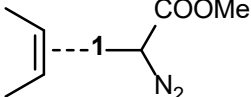
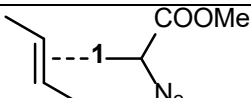
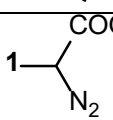
All stationary points were properly characterized by the correct number and nature of their imaginary frequencies. Mass-weighted Intrinsic Reactions Coordinate (IRC) [29,30] calculations were performed on transition states to obtain minima on both energy profile directions when necessary.

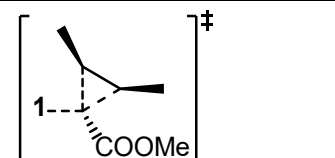
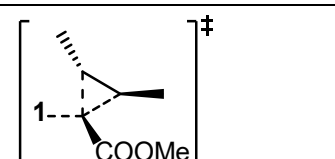
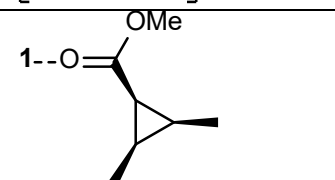
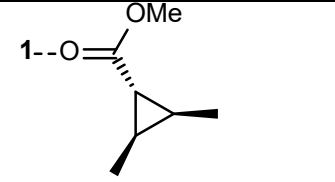
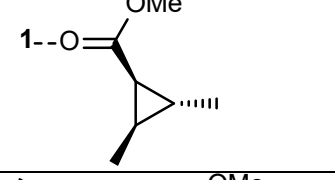
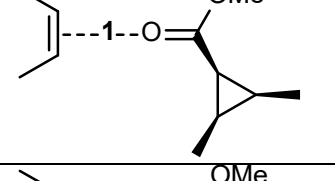
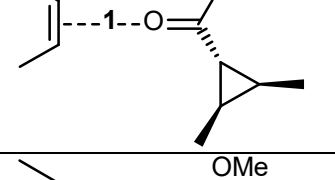
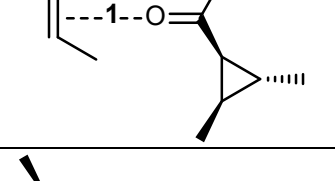
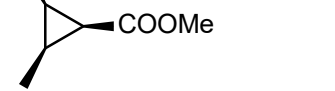


Solvent effects were computed through PCM model (solvent = acetonitrile or dichloromethane) by using the single-point energy calculations for some selected structures. However, results showed very little solvent effects (*ca.* 12 kJ mol<sup>-1</sup> as maximum). Differences between experimental results by using different reaction media would be thus attributed to the different solvent coordinating ability.

Unless otherwise stated, Gibbs free energies (by using non-scaled frequencies) are only used for the discussion on the relative stabilities of the considered chemical structures. The use of non-scaled frequencies on M06-2X calculations typically lead to a slight exaggeration of high vibrational frequencies and a slight underestimation of low vibrational frequencies [31].

Relative free energies (including thermal corrections at 25 °C) of the considered structures are shown in Table 1. Hard data on electronic, zero-point corrected and Gibbs free energies of all structures considered, are available in the Electronic Supplementary Material.

**Table 1** Numbering and relative Gibbs free energies (kJ mol<sup>-1</sup>) of the different structures considered in this work

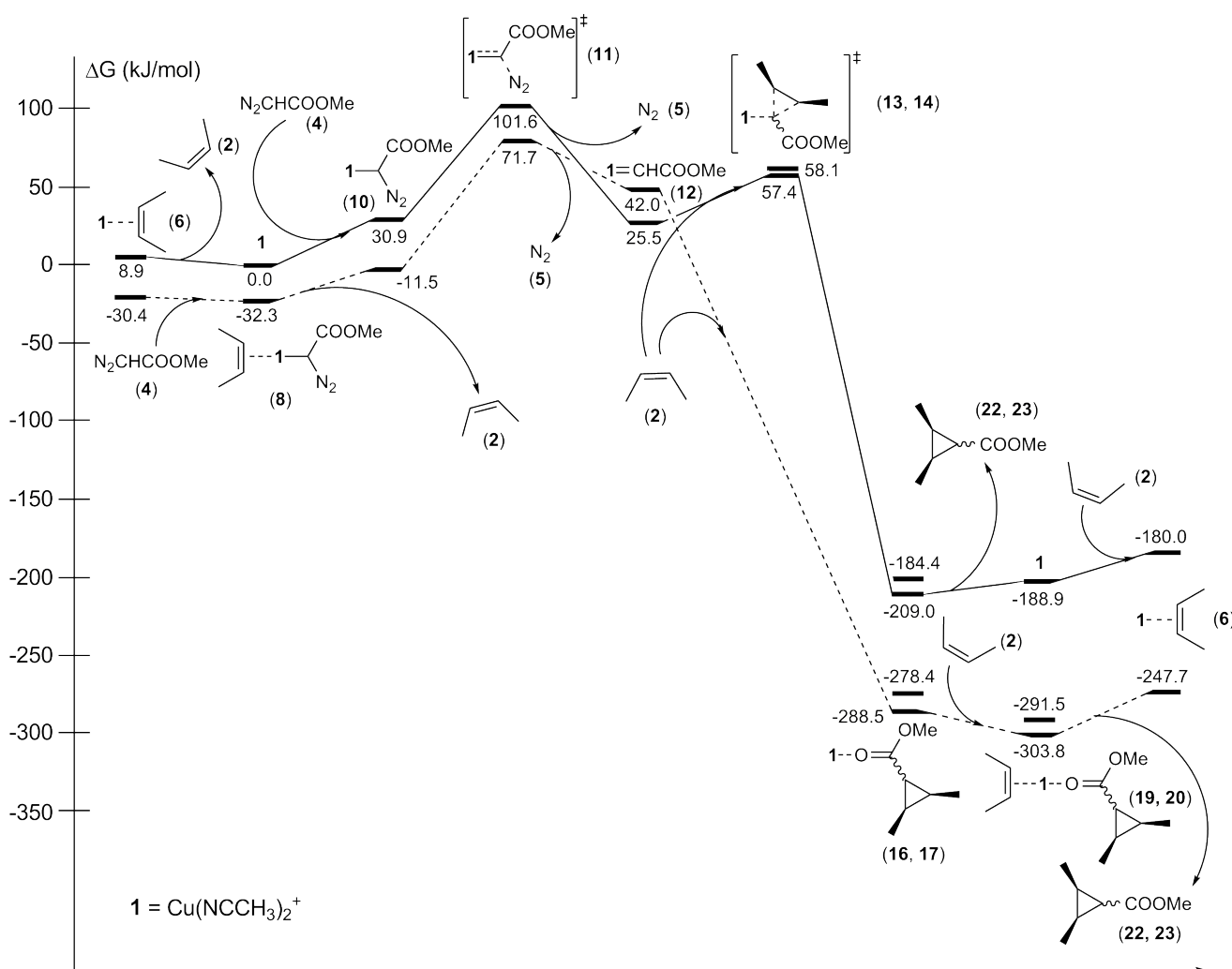
Schematic picture	Structure number	Relative energy (M06-2X)	Relative energy (O3LYP)
$\text{Cu}(\text{NCCH}_3)_2^+$	1	0	0
	2	0	0
	3	0	0
$\text{N}_2\text{CHCOOMe}$	4	0	0
$\text{N}_2$	5	0	0
1--- 	6	-30.4	8.9
1--- 	7	-29.6	11.0
	8	-32.3	Not found
	9	-34.2	Not found
1--- 	10	-11.5	30.9
$\left[ \begin{array}{c} \text{COOMe} \\   \\ \text{1} \\   \\ \text{N}_2 \end{array} \right]^\ddagger$	11	71.7	101.6
$\text{1}=\text{CHCOOMe}$	12	42.0	25.5
$\left[ \begin{array}{c} \text{COOMe} \\   \\ \text{1} \\   \\ \text{N}_2 \end{array} \right]^\ddagger$	13	Not found	57.4

	14	Not found	58.1
	15	Not found	60.1
	16	-278.4	-184.4
	17	-288.5	-209.0
	18	-293.8	-200.1
	19	-291.5	Not found
	20	-303.8	Not found
	21	-302.0	Not found
	22	-230.5	-169.0
	23	-247.7	-189.0
	24	-244.3	-180.7

### 3 Results and Discussion

#### 3.1 Formation of the Copper-Carbene Complex

The energy profile of the catalytic cycle for the Cu-catalyzed cyclopropanation reaction studied in this work is shown in Fig. 1, analogous to that reported for the ethylene reaction [11]. Energy profiles for the catalytic cycle of (*Z*)-but-2-ene (**2**) using both M06-2X and O3LYP functionals are displayed in Fig. 1 as well. A similar energy profile (not shown) has been obtained for the reaction of (*E*)-but-2-ene (**3**).



**Fig. 1** Energy profile of a catalytic cycle for (*Z*)-but-2-ene (**2**) by means of M06-2X (dashed line) and O3LYP (solid line) calculations

The relative free energies of the structures shown in the diagrams (in  $\text{kJ mol}^{-1}$ ) take into account the evolution of the system composition according to the different molecules entering or leaving the system. As shown in Table 1, the catalyst (**1**), (*Z*)-butene (**2**), methyl diazoacetate (**4**), and dinitrogen (**5**) have been

arbitrarily chosen as reference points for the calculation of relative free energies. The catalyst-butene complex (**6**) is gathered in Fig. 1 as both the starting structure and the final species of the energy profile, the energy difference ( $-188.9 \text{ kJ mol}^{-1}$  for M06-2X;  $-217.3 \text{ kJ mol}^{-1}$  for O3LYP) corresponding to the Gibbs free energy variation for a catalytic cycle, in good agreement with the irreversible character of cyclopropanation reactions.

Nonetheless, it is probably more noticeable that the reaction mechanism for the transformation of the catalyst-butene complex (**6**) into the catalyst-diazo compound species (**10**) changes depending on the calculation method used. At M06-2X level an associative displacement mechanism is slightly favored, where the exchange of butene by the diazo ester takes place through a butene-catalyst-methyl diazoacetate complex (**8**), which is stabilized by  $1.9 \text{ kJ mol}^{-1}$  relative to the former intermediate **6**, and the formation of the catalyst-methyl diazoacetate species (**10**) requires an energy increase of  $19.9 \text{ kJ mol}^{-1}$ .

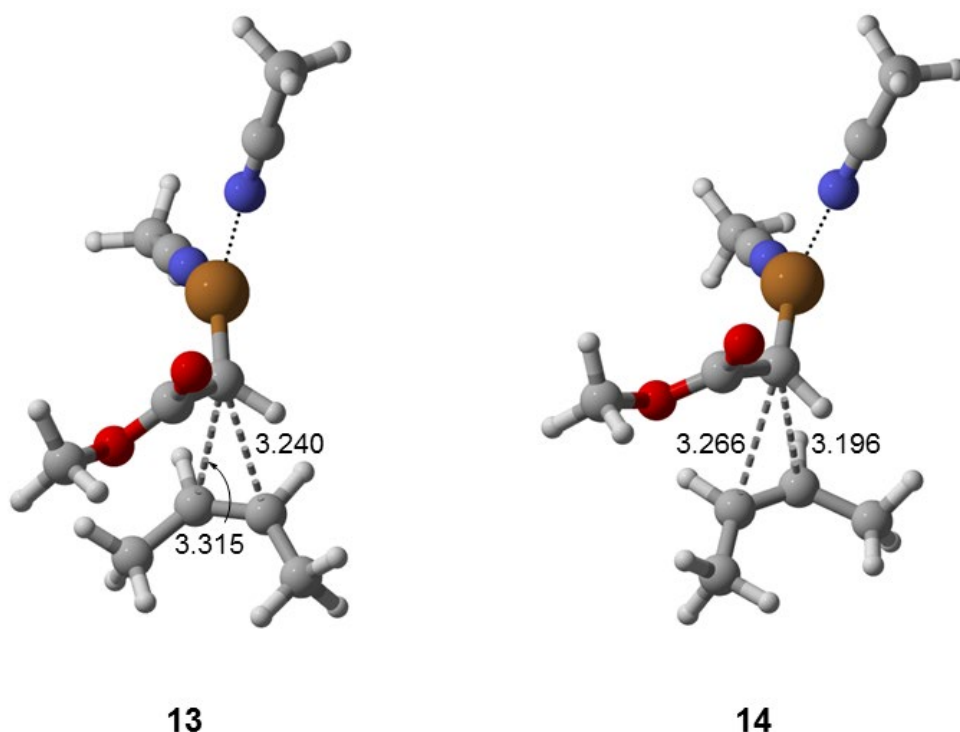
Since all the attempts for locating stationary points for tetrahedral structures **8** and **9** using O3LYP were unsuccessful, only a dissociative mechanism is consistent at this level for the transformation of **6** into **10**. This dissociative mechanism involves the formation of the naked catalyst, which can now coordinate to the diazo compound. The regeneration of the free catalyst is slightly favored (by  $8.9 \text{ kJ mol}^{-1}$ ), while the subsequent addition of the diazo ester is disfavored by  $30.9 \text{ kJ mol}^{-1}$ . Nevertheless, the trend is inverted when electronic energies are considered: the regeneration of the catalyst requires  $33.3 \text{ kJ mol}^{-1}$ , whereas the coordination of methyl diazoacetate is slightly favored by  $1.2 \text{ kJ mol}^{-1}$ .

The catalyst-methyl diazoacetate complex (**10**) can extrude dinitrogen (**5**) through TS **11** to yield a copper-carbene complex (**12**). The activation barrier for the overall process (i.e., from the starting compounds of the catalytic cycle) backs up previous works, confirming that copper-carbene complex formation is the rate-limiting step of the reaction ( $\Delta G^\ddagger = 104.0 \text{ kJ mol}^{-1}$  for M06-2X;  $\Delta G^\ddagger = 92.7 \text{ kJ mol}^{-1}$  for O3LYP), also for the reaction of (*E*)-but-2-ene (**3**) ( $\Delta G^\ddagger = 105.9 \text{ kJ mol}^{-1}$  for M06-2X;  $\Delta G^\ddagger = 90.6 \text{ kJ mol}^{-1}$  for O3LYP) [9-11].

### 3.2 Formation of Cyclopropane Products. *cis/trans* Selectivity

As it can be observed in Fig. 1, no TS for the direct carbene insertion could be located on the PES for this system using M06-2X. In order to locate that TS on the actual extreme flat PES, very uncorrelated calculation methods were required [19,20]. Thus, TSs **13** and **14**, corresponding to the formation of catalyst-product complexes (**16** and **17**, respectively) from the copper-carbene complex (**12**), were located using the O3LYP functional. The activation barriers are  $31.9 \text{ kJ mol}^{-1}$  for the formation of **13** and  $32.7 \text{ kJ mol}^{-1}$  for **14** (whilst for (*E*)-but-2-ene the formation of **18** requires an energy increase of  $34.6 \text{ kJ mol}^{-1}$ ). It is worth noting the extreme flatness of the PES, since these barriers, starting from the isolated reactants, become negative ( $-9.1$  and  $-8.8 \text{ kJ mol}^{-1}$ ;  $-7.1 \text{ kJ mol}^{-1}$  for (*E*)-but-2-ene) when electronic energies are considered, and makes remarkable the fact of finding those in such a reactive system, i.e., with a highly electrophilic cationic ligand-Cu-carbene complex and a nucleophilic alkene such as but-2-ene. Comparison between the activation barriers for (*Z*)- and (*E*)-but-2-ene shows a higher reactivity for the former, which can be attributed to the larger steric strain loss.

The O3LYP method was chosen in order to reproduce the experimental results indicating the occurrence of a reaction intermediate leading to different stereoselectivities depending on the reaction conditions. As a consequence, the stereoselectivity of the process has been theoretically studied only by using the O3LYP functional. Almost identical electronic (by 0.2 kJ mol<sup>-1</sup>) and Gibbs free energies (by 0.7 kJ mol<sup>-1</sup>) are found for TSs **13** and **14**, in *cis* and *trans* approaches (Fig. 2) respectively, which have been obtained for the reaction between the bis(acetonitrile)-coordinated copper-carbene complex and (*Z*)-but-2-ene. Such a lack of stereoselectivity is consistent with experimental results (49:51, experimental details available in Supplementary Material) and can be attributed to the negligible steric interactions between the ester group and either methyl group from butene. A 3.613 Å distance is found for the closest ester oxygen-methyl carbon pair in TS **13**, in good agreement with the expected methyl-oxygen van der Waals distance (3.68 Å) [32]. Since steric interactions are reflected on geometrical changes [33], some differences between the formation bond lengths (3.315 Å and 3.240 Å for **13**, 3.266 Å and 3.196 Å for **14**) can also be found.



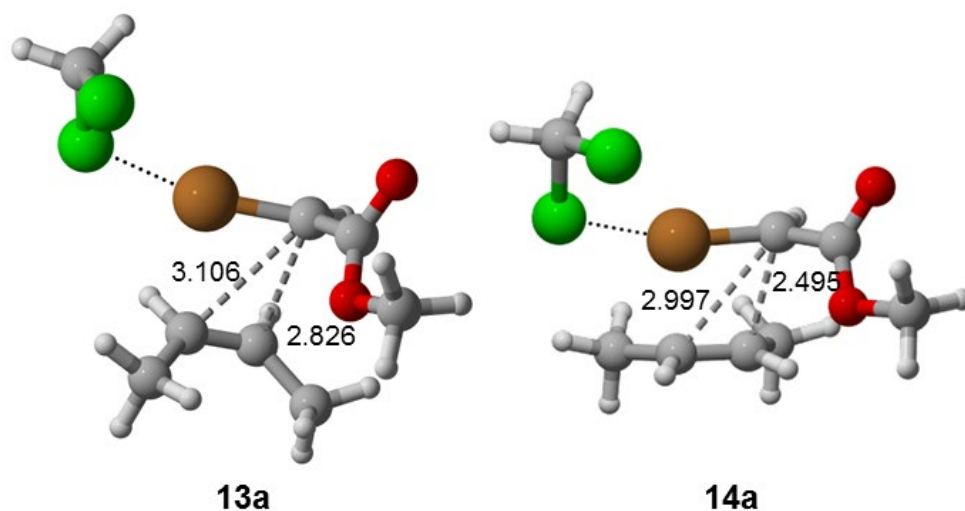
**Fig. 2** Transition states for the direct insertion from the bis(acetonitrile)-coordinated copper-carbene complex to (*Z*)-but-2-ene through *cis* (**13**) and *trans* (**14**) approaches

In order to assess the role of dispersion forces on the *cis/trans* selectivity, single point calculations were carried out for both *cis* and *trans* O3LYP-optimized TS's by using (or not) the empirical D3 Grimme correction by using a different functional (since O3LYP-D3 calculations are unavailable for Gaussian09). Thus, inclusion of dispersion M06-2X calculations leads to a very low preferential stabilization (by 0.3 kJ mol<sup>-1</sup>) of the *trans* TS.

In order to assess the role of the solvent on the reactivity, both TSs were recalculated by replacing both acetonitrile ligands by a dichloromethane molecule (TSs **13a** and **14a**, Fig. 3). Interestingly, a change in the coordination number of copper(I) ion (from 3 to 2) is found. Results also show a significant *trans*



preference in electronic energy terms (by 3.4 kJ mol<sup>-1</sup>), consistently with the experimental *trans/cis* selectivity (67/33, see Electronic Supplementary Material). Such a *trans* preference can be attributed to the closer positions between the ester group and both methyl olefin substituents, as indicated by the short lengths for the forming bonds (3.106 Å and 2.826 Å for **13a**; 2.977 Å and 2.495 Å for **14a**). Nevertheless, a low *trans* preference is found in Gibbs free energy terms (0.7 kJ mol<sup>-1</sup>), though the selectivity decrease induced by entropic effects is likely overestimated by gas-phase calculations [34].



**Fig. 3** Transition states for the direct insertion from the dichloromethane-coordinated copper-carbene complex to (*Z*)-but-2-ene through *cis* (**13**) and *trans* (**14**) approaches

The source of selectivity dependence on the ligand can be attributed to electrophilicity differences of the corresponding carbenes. Thus, a large increase of the negative Mulliken charge (-0.383) of the carbene carbon is found for the bis(acetonitrile)-coordinated carbene (**12**) when a further electron is added through single-point calculations, in contrast with the low variation for the dichloromethane-derived species (-0.054). The larger electrophilicity of the acetonitrile-derived carbene allows explaining the larger earliness of the corresponding TS's (hence, longer incipient C···C bonds), thus leading to weaker steric interactions.

On the other hand, the unsuccessfulness in locating minima for tetrahedral structures **19** and **20** with O3LYP leads to different mechanisms for the regeneration of the starting catalyst **6** from **16** or **17**, depending on the method: an associative pathway is preferred when M06-2X is used, where **22** (**23**) is formed through the coordination of a butene molecule to **16** (**17**), leading to **19** (**20**), with an energy stabilization of 15.3 kJ mol<sup>-1</sup>, which subsequently decoordinates a product molecule with an energy rise of 25.7 kJ mol<sup>-1</sup>. At O3LYP level, a dissociated pathway is only consistent with the calculations, in which the reaction product **22** (**23**) decoordinates to yield the naked catalyst and then occurs the coordination of the butene molecule. This process requires an energy increase of 29.0 kJ mol<sup>-1</sup>. The reaction products are methyl (1*s*,2*R*,3*S*)-2,3-dimethylcyclopropanecarboxylate (**22**, all-*cis*) and methyl (1*r*,2*R*,3*S*)-2,3-dimethylcyclopropanecarboxylate (**23**, COOMe-*trans*). Both (2*R*,3*R*) and (2*S*,3*S*) enantiomers of methyl 2,3-dimethylcyclopropanecarboxylate (**24**, methyl-*trans*) are the reaction products when (*E*)-but-2-ene is considered.

## 4 Conclusions

DFT calculations carried out in this study back up the current proposed mechanism so far, which is consistent with experimental data obtained for related systems. Assuming the catalyst-butene complex as the starting species for a catalytic cycle, two mechanisms are possible for the replacement of the olefin by the diazo ester, depending on the calculation method used: for M06-2X, an associative mechanism is preferred, whereas for O3LYP a dissociative mechanism is favored. The catalyst-diazo compound complex formed can extrude dinitrogen to yield a copper-carbene complex, being this process the rate-limiting step. It is noticeable the difference between both calculation methods in the calculated activation barrier on the PES.

Assuming a concerted mechanism for the formation of the cyclopropane ring (i.e. direct carbene insertion), the location of the TS controlling the stereoselectivity of the process has only been possible with the O3LYP functional, because of the extreme flatness of the PES in this area for this kind of systems. The increase of the *cis/trans* selectivity when two acetonitrile ligands are replaced by a dichloromethane molecule can be attributed to the decrease of the forming bond lengths in the corresponding TSs (hence, allowing a stereochemical discrimination).

The formation of the catalyst-product complex is greatly favored for the cyclopropanation step. The regeneration of the catalyst-ethylene complex can take place through an associative displacement if M06-2X is used, while a dissociative displacement is preferred with O3LYP.

In conclusion, a thorough examination of the PES of the model reaction studied with two different functionals has proved that, although minor differences are found at some points of the mechanism of copper-catalyzed cyclopropanation reactions between them, both describe qualitatively and reasonably well the key steps of the process. Moreover, *cis/trans* selectivity has been theoretically studied by terms of O3LYP for a representative model, and is in qualitative agreement with the experimental data.

## References

1. Salaün J (2000) *Top Curr Chem* 207:1-67. Doi:10.1007/3-540-48255-5\_1
2. Kulinkovich OG (2015) *Cyclopropanes in Organic Synthesis*. Wiley, Hoboken, NJ. Doi: 10.1002/9781118978429
3. Lebel H, Marcoux J-F, Molinaro C, Charette AB (2003) *Chem Rev* 103:977-1050. Doi: 10.1021/cr010007e
4. Pellissier H (2008) *Tetrahedron* 64:7041-7095. Doi: 10.1016/j.tet.2008.04.079
5. Bartoli G, Bencivenni G, Dalpozzo R (2014) *Synthesis* 46:979-1029. Doi: 10.1055/s-0033-1340838
6. García JI, Salvatella L, Pires E, Fraile JM, Mayoral JA (2014) In: Knochel A, Holander GA (ed) *Comprehensive Organic Synthesis II*. Elsevier, Amsterdam. Doi: 10.1016/B978-0-08-097742-3.00426-2
7. Charette AB, Lebel H, Roy M-N (2014) In: Alexakis A, Krause N, Woodward S (ed) *Copper-Catalyzed Asymmetric Synthesis* Wiley-VCH Verlag, Weinheim. Doi: 10.1002/9783527664573.ch8
8. Besora M, Braga AAC, Sameera WMC, Urbano J, Fructos MR, Pérez PJ, Maseras F (2015) *J Organomet Chem* 784:2-12. Doi: 10.1016/j.jorganchem.2014.10.009
9. Salomon RG, Kochi JK (1973) *J Am Chem Soc* 95:3300-3310. Doi: 10.1021/ja00791a038
10. Díaz-Requejo MM, Belderrain TR, Nicasio MC, Prieto F, Pérez PJ (1999) *Organometallics* 18:2601-2609. Doi: 10.1021/om990270u
11. Fraile JM, García JI, Martínez-Merino V, Mayoral JA, Salvatella L (2001) *J Am Chem Soc* 123:7616-7625. Doi: 10.1021/ja003695c

12. Fraile JM, García JI, Gissibl A, Mayoral JA, Pires E, Reiser O, Roldán M, Villalba I (2007) *Chem Eur J* 13:8830-8839. Doi: 10.1002/chem.200700681.
13. Straub BF, Gruber I, Rominger F, Hofmann P (2003) *J Organomet Chem* 684:124-143. Doi: 10.1016/S0022-328X(03)00520-5
14. Özen C, Tüzün NŞ (2008) *Organometallics* 27:4600-4610. Doi: 10.1021/om800094k
15. Meng Q, Li M, Tang D, Shen W, Zhang J (2004) *J Mol Struct (THEOCHEM)* 711: 193-199. Doi: 10.1016/j.theochem.2004.06.050
16. Drudis-Solé G, Maseras F, Lledós A, Vallibera A, Moreno-Mañas M (2008) *Eur J Org Chem* 2008:5614-5621. Doi: 10.1002/ejoc.200800762
17. Rasmussen T, Jensen JF, Østergaard N, Tanner D, Ziegler T, Norrby P-O (2002) *Chem Eur J* 8:177-184. Doi: 10.1002/1521-3765(20020104)8:1<177::AID-CHEM177>3.0.CO;2-H
18. García JI, Jiménez-Osés G, Mayoral JA (2011) *Chem Eur J* 17:529-539. Doi: 10.1002/chem.201001262
19. Cohen AJ, Handy NC (2001) *Mol Phys* 99:607-615. Doi: 10.1080/00268970010023435
20. Handy NC, Cohen AJ (2001) *Mol Phys* 99:403-412. Doi: 10.1080/00268970010018431
21. Fraile JM, García JI, Herrerías CI, Pires E (2017) *Synthesis*, 49: 1444-1460. Doi: 10.1055/s-0036-1588699
22. Angulo B, Fraile JM, Herrerías CI, Mayoral JA (2017) *RSC Adv* 7:19417-19424. Doi: 10.1039/c7ra01017f
23. Liang HC, Kim E, Incarvito CD, Rheingold AL, Karlin KD (2002) *Inorg Chem* 41:2209-2212. Doi: 10.1021/ic010816g
24. Frisch MJ, Trucks GW, Schlegel HB, Scuseria GE, Robb MA, Cheeseman JR, Scalmani G, Barone V, Mennucci B, Petersson GA, Nakatsuji H, Caricato M, Li X, Hratchian HP, Izmaylov AF, Bloino J, Zheng G, Sonnenberg JL, Hada M, Ehara M, Toyota K, Fukuda R, Hasegawa J, Ishida M, Nakajima T, Honda Y, Kitao O, Nakai H, Vreven T, Montgomery JA Jr, Peralta JE, Ogliaro F, Bearpark M, Heyd JJ, Brothers E, Kudin KN, Staroverov VN, Kobayashi R, Normand J, Raghavachari K, Rendell A, Burant JC, Iyengar SS, Tomasi J, Cossi M, Rega N, Millam JM, Klene M, Knox JE, Cross JB, Bakken V, Adamo C, Jaramillo J, Gomperts R, Stratmann RE, Yazyev O, Austin AJ, Cammi R, Pomelli C, Ochterski JW, Martin RL, Morokuma K, Zakrzewski VG, Voth GA, Salvador P, Dannenberg JJ, Dapprich S, Daniels AD, Farkas Ö, Foresman JB, Ortiz JV, Cioslowski J, Fox DJ (2009) *Gaussian 09, Revision A.02*. Gaussian, Wallingford, CT
25. Frisch MJ, Trucks GW, Schlegel HB, Scuseria GE, Robb MA, Cheeseman JR, Scalmani G, Barone V, Mennucci B, Petersson GA, Nakatsuji H, Caricato M, Li X, Hratchian HP, Izmaylov AF, Bloino J, Zheng G, Sonnenberg JL, Hada M, Ehara M, Toyota K, Fukuda R, Hasegawa J, Ishida M, Nakajima T, Honda Y, Kitao O, Nakai H, Vreven T, Montgomery JA Jr, Peralta JE, Ogliaro F, Bearpark M, Heyd JJ, Brothers E, Kudin KN, Staroverov VN, Keith T, Kobayashi R, Normand J, Raghavachari K, Rendell A, Burant JC, Iyengar SS, Tomasi J, Cossi M, Rega N, Millam JM, Klene M, Knox JE, Cross JB, Bakken V, Adamo C, Jaramillo J, Gomperts R, Stratmann RE, Yazyev O, Austin AJ, Cammi R, Pomelli C, Ochterski JW, Martin RL, Morokuma K, Zakrzewski VG, Voth GA, Salvador P, Dannenberg JJ, Dapprich S, Daniels AD, Farkas Ö, Foresman JB, Ortiz JV, Cioslowski J, Fox DJ (2013) *Gaussian 09, Revision D.01*. Gaussian, Wallingford, CT
26. Zhao Y, Truhlar DG (2008) *Theor Chem Acc* 120:215-241. Doi: 10.1007/s00214-007-0310-x
27. Bozic-Weber B, Chaurin V, Constable EC, Housecroft CE, Meuwly M, Neuburger M, Rudd JA, Schönhofer E, Siegfried L (2012) *Dalton Trans* 41:14157-14169. Doi: 10.1039/C2DT31159C
28. Tamasi G, Bonechi C, Rossi C, Cini R, Magnani A (2016) *J Coord Chem* 69:404-424. Doi: 10.1080/00958972.2015.1132416
29. Gonzalez C, Schlegel HB (1990) *J Phys Chem* 94:5523-5527. Doi: 10.1021/j100377a021
30. Gonzalez C, Schlegel HB (1989) *J Chem Phys* 90:2154-2161. Doi: 10.1063/1.456010
31. Laury ML, Carlson MJ, Wilson AK (2012) *J Comp Chem* 33: 2380-2387. Doi: 10.1002/jcc.23073
32. Hu S-Z, Zhou, Z-H, Xie Z-X, Robertson B E (2014) *Z Kristallogr* 229: 517-523. Doi: 10.1515/zkri-2014-1726
33. Stojanović M, Aleksić J, Baranac-Stojanović M (2015) *Tetrahedron* 71: 5119-5123. Doi: 10.1016/j.tet.2015.06.22
34. Leung BO, Reid DL, Armstrong DA, Rauk A (2004) *J Phys Chem A* 108: 2720-2725. Doi: 10.1021/jp030265a